A Multivariate Curve Resolution Approach to the Study of the Degradation Kinetics of Valsartan under Photolytic and Acid Conditions

ROMINA M. BIANCHINI, TEODORO S. KAUFMAN

Pharmaceutical Analysis, School of Biochemical and Pharmaceutical Sciences, National University of Rosario and Institute of Chemistry of Rosario, Rosario S2002LRK, *Argentina*

Received 22 March 2013; revised 5 June 2013; accepted 5 June 2013

DOI 10.1002/kin.20808
Published online 28 August 2013 in Wiley Online Library (wileyonlinelibrary.com).

ABSTRACT: The analysis of UV-spectrophotometric data with second-order chemometrics techniques, including multivariate curve resolution with alternating least-squares (MCR-ALS) and hybrid hard- and soft MCR (HS-MCR), was examined as an alternative tool for studying the kinetics of drug degradation under stress conditions, employing valsartan (VAL) as a model drug. Despite small structural and spectroscopic differences between VAL and its degradation products, MCR-ALS and HS-MCR were able to detect the generation of two photoneutral degradation products (DP-1 and DP-2) and a single acid hydrolysis product (DP-3), providing good approximations to their pure spectra and concentration profiles, from which estimations of the kinetic profiles and rate constants were obtained. Kinetic models based on first-order reactions explained the degradation processes. MCR-ALS and HS-MCR analyses yielded similar rate constants; however, the latter was capable of more properly fitting the experimental data to a kinetic model in the case of drug photolysis. The results were confirmed by comparison with data obtained by HPLC analysis of the degraded samples. Int J Chem Kinet 45: 734–743, 2013

INTRODUCTION

Spectrophotometric techniques are largely used in the field of analytical chemistry because of the ease of spectral data acquisition, handling, and interpretation. In addition, they are highly sensitive and very suitable for studying chemical reactions in a solution. Most conventional spectrophotometric methods are able to furnish results employing a discrete number of wavelengths; however, these are not enough by themselves to uncover the information required to solve systems with severe spectral overlapping.

Correspondence to: Teodoro S. Kaufman; e-mail: kaufman@iquir-conicet.gov.ar

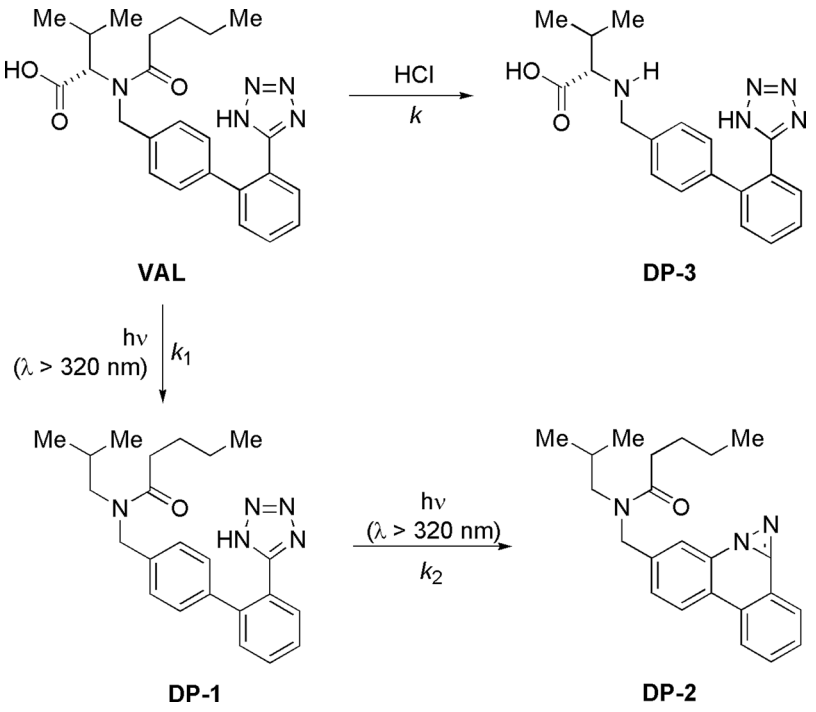

Scheme 1 Degradation of VAL under photolytic (DP-1 and DP-2) and acid (DP-3) conditions.

In recent years, chemometric approaches have been proposed as an useful strategy for the extraction of analytical information from multivariate data [1,2]. These methods advantageously exploit full spectral information, by using simultaneously all measured analytical signals. Multivariate curve resolution (MCR) methods are second-order chemometric tools suitable for the analysis of the dynamics of complex systems, due to their ability to provide detailed information concerning the spectra of the involved components together with their concentration profiles [3,4].

Drug degradation represents a serious problem, which relates to loss of the pharmacological activity and the possibility of production of adverse effects induced by the resulting degradation impurities [5]. Accordingly, the International Conference on Harmonization (ICH) guidelines require to carry out stress tests on drug substances and drug products to acquire a better understanding of the intrinsic stability of drugs, as well as knowledge on the nature of the degradation products and the operating degradation mechanisms [6]. These tests also generate useful information to improve manufacturing processes and to select the proper packaging [7].

Valsartan (VAL, Scheme 1) is a synthetic nonpeptidic compound with angiotensin receptor blocking activity, which binds selectively and noncompetitively to the type-1 angiotensin II receptors, preventing the action of angiotensin II. The drug is widely used for treatment of hypertension [8].

Stress tests demonstrated that VAL suffers relevant degradation when exposed to photolytic and acidic conditions [9–12]. The outcome of the photodegradation is often influenced by the source of light and its intensity, as well as the reaction solvent and the extent of the exposure. Under our experimental conditions, the photoneutral degradation products were identified as *N*-[2′-(1*H*-tetrazol-5-yl)-biphenyl-4-ylmethyl]-*N*-isobutylpentanamide (DP-1) and *N*-(diazirino[1,3-*f*]phenanthridin-4-ylmethyl)-*N*-isobutylpentanamide (DP-2) [13]. The latter are structurally related to those found by the group of Singh [12], and their structures have been unequivocally determined after exhaustive analyses of their NMR spectra and other analytical methods [13]. On the other hand, the structure of the acid degradation product (DP-3) has been elucidated as (*S*)-2-{*N*-(2′-(1*H*-tetrazol-5-yl)biphenyl-4-yl)methyl}-3-methylbutanoic acid (Fig. 1) [14], which results from the hydrolytic cleavage of the amide bond. The pathways of formation of the impurities have been discussed elsewhere [13].

Therefore, herein we examine the suitability of multivariate curve resolution with alternating least-squares (MCR-ALS) and the hybrid hard–soft multivariate curve resolution (HS-MCR) modeling method,

for studying the kinetics of the acid and photoneutral degradation of VAL bulk drug by analysis of UV spectrophotometric data. Comparison with an independent HPLC procedure allowed assessment of the results provided by the chemometrics methods.

EXPERIMENTAL

Instrumentation, Chemicals, and Materials

Light exposure was performed in a 55 cm × 45 cm × 30 cm photostability chamber fitted with a 400 W metal halide lamp (Philips Lighting, Turnhout, Belgium) emitting light mainly between 320 and 400 nm (radiation flux at 1.00 m = 1000 $\mu W/cm^2$). The UV spectra were acquired using a Shimadzu 1650PC double beam spectrophotometer driven by UV-Probe v.1.1 software. For acquisition of the spectra, the samples were continuously withdrawn from the reaction vessels by means of a Gilson Minipuls 3 peristaltic pump, passed through an 80-μL flow cell (Hellma, 10 mm optical path) and returned to the vessels.

The reaction vessel was thermostated to ±0.2°C employing a Thermolyne constant temperature bath. Inner-vessel temperatures were determined with a DigiSense digital thermometer, fitted with a J-type thermocouple.

The HPLC analyses were carried out with a Varian Prostar 210 liquid chromatograph (Varian, Walnut Creek, CA) equipped with two isocratic pumps, a Rheodyne injector fitted with a 20-μL loop, a 250 mm × 4.6 mm cyano column (Luna, 5 μm particle size), a temperature controller set at 30°C, and Varian Prostar 325 variable dual-wavelength UV–vis detector set at 226 nm. Elution was performed with a 40:60 (v/v) mixture of acetonitrile (ACN) and potassium phosphate solution (20 mm, pH 3.0), pumped at a flow rate of 1.0 mL min^{-1}. Solvents were degassed with a Branson 1200 ultrasonic cleaner. The chromatograms were recorded and analyzed employing Varian Galaxie v.6.0 software.

The chemometrics computations were performed in Matlab v.7.4 (Mathworks, Natwick, MA) employing the MCR-ALS user-friendly interface tool [15]. Graphics were processed with Origin Pro v.8.0 (OriginLab, Northampton, MA).

The experiments were performed with pharmaceutically certified VAL and analytical-grade reagents (Merck, Darmstadt, Germany). Aqueous solutions were prepared employing double distilled water. HPLC-grade solvents (J. T. Baker, Mexico City, Mexico) were employed for the chromatographic analyses and for sample preparation. A stock solution of VAL (0.532 mg mL^{-1}) was prepared in water:^{t}BuOH (4:1, v/v) by dissolution of an accurately weighed amount of the drug in ^{t}BuOH, completing to the mark with water. Phosphate solutions and standardized HCl solutions were prepared according to USP 32 [16]. Liquids were filtered through 0.45 μm nylon membranes before use.

Degradation under Photolytic Conditions

An aliquot of the stock solution of VAL was diluted with degassed water to a final concentration of 0.063 mg mL^{-1}. The solution was transferred to a reaction cell, placed at 15 cm from the source, and irradiated at 25°C. UV spectra were recorded between 230 and 300 nm, every 4 min.

For the comparative HPLC study, a solution of VAL (0.089 mg mL^{-1}) was similarly irradiated. Samples (0.5 mL) were periodically withdrawn and injected in the chromatograph [11] without further treatment.

Degradation under Acid Conditions

The experiments were performed according to ICH recommendations for drug stability tests [7]. Aliquots (2.0 mL) of the stock solution of VAL were diluted with 1.88 N HCl (samples A and C) and with 0.73 N HCl (sample B) to a final concentration of 0.035 mg mL^{-1}. Samples A and B were treated at 85.0°C (358 K), whereas sample C was degraded at 65.0°C (338 K). UV spectra were recorded between 220 and 260 nm at 1.0 min intervals during 3 h for samples A and C and for 4 h for sample B.

For the comparative HPLC analyses, solutions of VAL (4.00 mg mL^{-1}) in 0.4942 N HCl were heated at 42 and 100°C (315 and 373 K) and a solution of VAL (4.00 mg mL^{-1}) in 0.1050 HCl was treated at 100°C. Aliquots (0.5 mL) were periodically withdrawn, carefully neutralized with 0.1 N NaOH, diluted to 5.0 mL with the mobile phase, and injected in the chromatograph [11].

Theoretical Background

Boldface capital letters are used for matrices, boldface lowercase characters are employed for vectors, and lowercase italics are used for scalars. A transposed matrix is indicated by a superscript "T," and $\| \mathbf{X} \|$ stands for the norm of matrix $\mathbf{X}$.

MCR-ALS

When a degradation process is monitored by UV spectroscopy, a series of spectra are collected as a function of time, containing the contributions from the n components acquired at the different wavelengths. The spectral changes that take place during the studied process can be used by MCR-ALS or HS-MCR to extract the analytical information required to solve the system, including the spectra of the individual components and their concentration profiles.

To that end, these spectroscopic measurements should be ordered in a data matrix $\mathbf{D}_{(r \times c)}$, whose rows contain the spectra acquired at different times (r) and whose columns are the process signals (absorbances) at different wavelengths (c). Assuming an additive linear model, the MCR-ALS algorithm seeks the optimal decomposition of the data matrix $\mathbf{D}_{(r \times c)}$ into the product of matrices $\mathbf{C}$ and $\mathbf{S}^{\mathrm{T}}$ according to Eq. (1) [17,18], from initial estimates of either one of them. Matrix $\mathbf{C}$ contains concentration information of the n sample components of the system, $\mathbf{S}$ is the matrix of their pure spectra, and $\mathbf{E}$ contains the model error:

$$\mathbf{D}_{(r \times c)} = \mathbf{C}_{(r \times n)}\mathbf{S}^{\mathrm{T}}_{(n \times c)} + \mathbf{E}_{(r \times c)} \tag{1}$$

In the MCR-based methods, the first step is the estimation of the number of components (n) involved, which can be initially obtained by application of the singular value decomposition [19]. MCR-ALS also needs a preliminary estimation of $\mathbf{S}^{\mathrm{T}}$ or $\mathbf{C}$, which is provided either by evolving factor analysis [20], by selection of the pure variables [21], or by any previous estimation of them. The spectra of standards of the components, when available, are also suitable to preliminary estimate $\mathbf{S}^{\mathrm{T}}$.

Given the initial estimates of matrices $\mathbf{C}$ or $\mathbf{S}^{\mathrm{T}}$, the ALS algorithm executes a constrained optimization process [22]. It carries out the decomposition of matrix **D,** given in Eq. (1), to iteratively try to find a model able to minimize the residual sum of squares (rss), employed as an error criterion Eq. (2).

To that end, ALS iteratively solves two alternating least-squares problems, the minimization of rss over $\mathbf{C}$ for a fixed $\mathbf{S}$ and the minimization of rss over $\mathbf{S}$ for a fixed $\mathbf{C}$ (Eqs. (3) and (4)), calculating new estimations of $\mathbf{S}^{\mathrm{T}}$ and $\mathbf{C}$ at the end of each cycle [23]. It does so until rss reaches a minimum value. Because of rotational ambiguities, constraints must be added to ensure that the mathematical solutions found by the iteration process are also chemically sound [24]:

$$\mathrm{rss} = \|\mathbf{E}\| = \left\|\mathbf{D} - \mathbf{C}\mathbf{S}^{\mathrm{T}}\right\| \tag{2}$$

$$\mathrm{Min}\,(\mathbf{C}) \left\|\mathbf{D} - \mathbf{C}\mathbf{S}^{\mathrm{T}}\right\| \rightarrow \mathbf{C} = \mathbf{D}\mathbf{S}\left(\mathbf{S}^{\mathrm{T}}\mathbf{S}\right) \tag{3}$$

$$\mathrm{Min}\left(\mathbf{S}^{\mathrm{T}}\right) \left\|\mathbf{D} - \mathbf{C}\mathbf{S}^{\mathrm{T}}\right\| \rightarrow \mathbf{S} = \mathbf{D}^{\mathrm{T}}\mathbf{C}\left(\mathbf{C}^{\mathrm{T}}\mathbf{C}\right)^{-1} \tag{4}$$

The iteration procedure ends after completion of a preselected number of cycles or when the percentage of lack of fit (%LOF) does not change significantly between consecutive iterations and convergence is achieved. The explained variance (r^2) is indicative of the quality of MCR-ALS modeling results [25].

Hard–Soft Multivariate Curve Resolution

The hard–soft multivariate curve resolution (HS-MCR) procedure introduces a previously selected kinetic model as a new constraint. In addition to spectral and concentration profiles, this method yields rate constants information [26].

By constraining the system with a preselected kinetic model, the HS-MCR algorithm is able to overcome some of the limitations of pure hard and pure soft modeling of dynamic processes. Particularly, HS-MCR is able to minimize the rotational ambiguity associated with the estimation of the concentration profiles when only nonnegativity and closure constraints are used [23], allowing a better estimation of the kinetic constants associated with the postulated model.

RESULTS AND DISCUSSION

Chemometrics Exploration of the Photodegradation of VAL

Figure 1 exhibits the spectral data acquired during the photodegradation of VAL. When the data matrix was

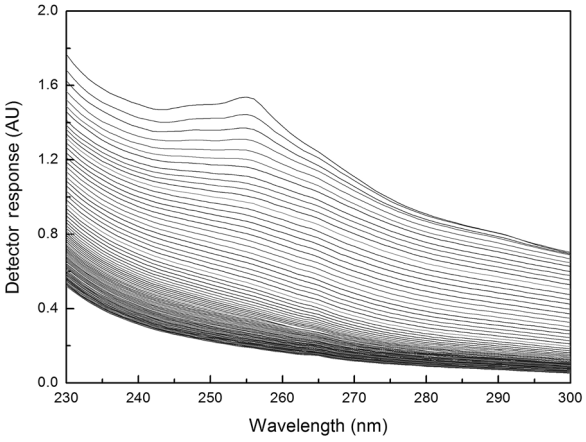

Figure 1 UV spectra of the photodegradation of VAL (0.063 mg mL^{-1}) at room temperature.

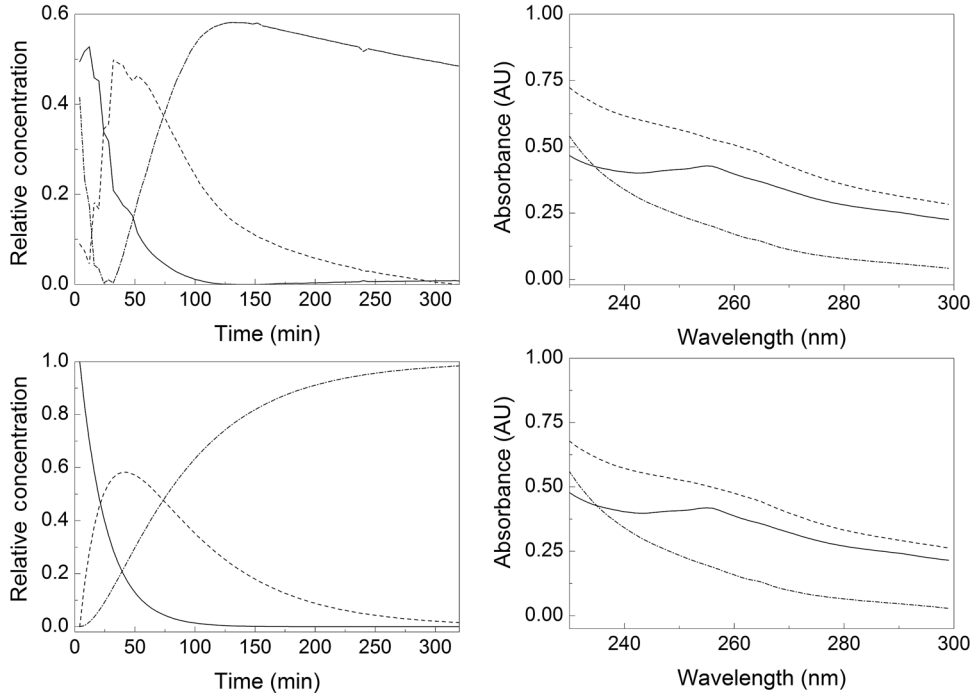

Figure 2 Resolved kinetic profiles (left) and pure spectra (right) of VAL (—), DP-1 (– –), and DP-2 (–•–) from the photodegradation of VAL. Top: MCR-ALS; bottom: HS-MCR.

processed by the MCR-ALS algorithms using nonnegativity (concentrations and spectra of the components must be positive) and closure (mass balance should be maintained during the kinetic process) constraints [27], the presence of three species (%LOF = 3.88%) was uncovered. From the resulting spectral and concentration profiles, it was deduced that the initial formation of an intermediate takes place, concomitant with decreasing absorbance of the solution; in turn, this is further degraded into a second product.

Figure 2 shows their calculated concentration profiles and relative pure spectra. Previous knowledge of the system allowed the assignment of structures DP-1 and DP-2 to the initial intermediate and the second product, respectively, as shown in Scheme 1.

Interestingly, despite exhibiting some imprecision in estimation of the concentrations of the degradation products during the first part of the experiment, MCR-ALS was capable of distinguishing the presence of intermediate DP-1, which spectral shape is not too different from that of VAL.

The evolution of the concentration profiles of VAL and both degradation products was in agreement with a kinetic model involving two consecutive first-order reactions, where k_1 and k_2 are their corresponding rate constants (Scheme 1). This was confirmed by the use of the HS-MCR technique, which adjusted the data to Eqs. (5) and (6) [28]. Both MCR-ALS and HS-MCR yielded similar $t_{1/2}$ values for the degradation of VAL; however, calculation of k_2 by MCR-ALS was troublesome, whereas HS-MCR provided comparatively less noisy models:

$$[\mathrm{DP}-1]_t = \frac{[\mathrm{VAL}]_0}{1-k_2/k_1} * \left(\mathrm{e}^{-k_2 t} - \mathrm{e}^{-k_1 t}\right) \qquad (5)$$

$$[\mathrm{DP}-2]_t = [\mathrm{VAL}]_0 * \left(1-\mathrm{e}^{-k_1 t}\right) - \frac{[\mathrm{VAL}]_0}{1-k_2/k_1} * \left(\mathrm{e}^{-k_2 t} - \mathrm{e}^{-k_1 t}\right) \qquad (6)$$

The rate constants, half-lives, and fitted parameters obtained for the photodegradation process are summarized in Table I.

MCR-ALS Analysis of the Degradation of VAL in Acid Medium

Figure 3 shows the overlain spectra obtained from the degradation of VAL, between 220 and 260 nm, when the drug was exposed to different temperatures and acid concentrations. The spectral profiles observed in the three cases are barely different, exhibiting a slight

Table I Kinetic Parameters of the Photodegradation of VAL[a]

Method	k_1 (min/min^{-1})	$t_{1/2}$ (min)	k_2 (min^{-1})	LOF (%)	r^2
MCR-ALS	0.042 (1)	16.7	[b]	3.88	0.9985
HS-MCR	0.044 (2)	15.8	0.015 (5)	5.38	0.9971
HPLC	0.045 (2)	15.5	0.022 (5)		0.9981 (k_1)
					0.9859 (k_2)

[a]Numbers in parentheses indicate the standard deviations of the determinations at the last significant digits level.
[b]Determination of k_2 employing this method was troublesome, yielding unreliable results.

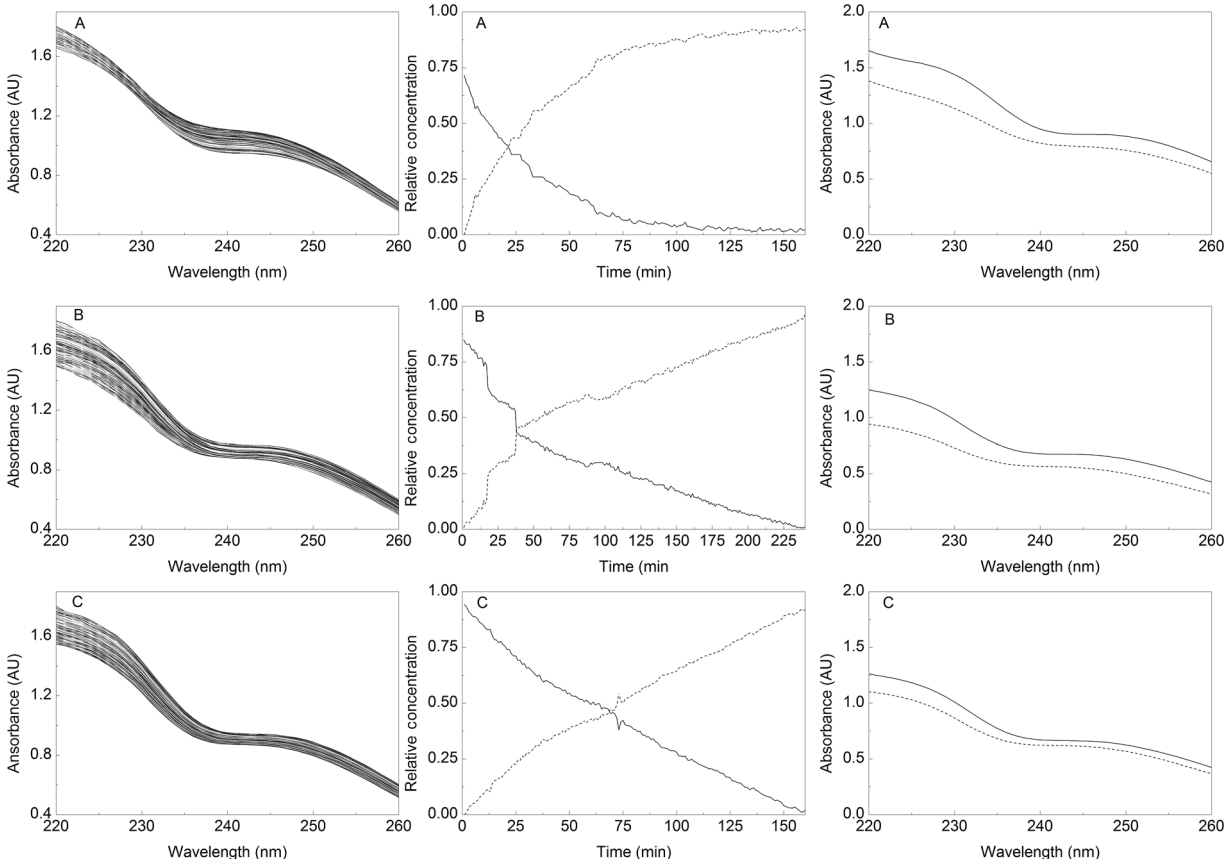

Figure 3 Acid degradation experiments of VAL (0.035 mg mL^{-1}). (A) In 1.88 N HCl at 85°C; (B) In 0.73 N HCl at 85 °C; (C) In 1.88 N HCl at 65°C. Left: UV spectra between 220 and 280 nm. Center: MCR-ALS resolved kinetic profiles of VAL (—) and DP-3 (– –) obtained in the acid degradation experiments of samples of VAL (0.035 mg mL^{-1}). Right: MCR-ALS resolved spectral profiles of VAL (—) and DP-3 (– –).

decrease of absorbance during the reaction course. In addition and not unexpectedly, it was observed that increasing acid concentration and/or the temperature accelerated the hydrolytic process.

When the experimental data were processed by the MCR-ALS procedure employing nonnegativity and concentration closure constraints, only two species were found, to which the identities of VAL and DP-3 were assigned, based on previous experience (Scheme 1) [11,13]. Their calculated concentration profiles and relative pure spectra are shown in Fig. 3.

The %LOF values of the deconvolutions were below 1.1% in all cases, and the resulting spectral shapes of the samples' components, which were in good agreement with those of authentic samples [13], did not show significant differences among the experiments. In addition, the evolution of the concentration profile plots was in agreement with a first-order kinetic model (Eq. (7), where $[VAL]_0$ and $[VAL]_t$ are the

Table II MCR-ALS and HS-MCR Derived Parameters, Characterizing the Acid-Catalyzed Degradation Kinetics of VAL under Different Conditions[a]

Condition		MCR-ALS				HS-MCR			
HCl (N)	T (°C)	k (min^{-1})	$t_{1/2}$ (min)	LOF (%)	r^2	k (min^{-1})	$t_{1/2}$ (min)	LOF (%)	r^2
1.88	85.0	0.0297 (2)	23.3	0.19	0.9964	0.0240 (2)	28.9	1.08	0.9999
1.88	65.0	0.0127 (1)	54.6	0.11	0.9948	0.01000 (5)	69.3	0.19	0.9999
0.73	85.0	0.01065 (4)	65.1	0.24	0.9988	0.00966 (7)	71.7	1.08	0.9999
E_a			10.2 kcal mol^{-1}				10.4 kcal mol^{-1}		

[a]Numbers in parentheses indicate the standard deviations of the determinations at the last significant digits level.

concentrations of VAL at the beginning of the experiment and at time t, respectively. The rate constants (k) and half-lives ($t_{1/2}$) of the process (Eq. (8), corresponding to the amide bond cleavage with the loss of the pentanoyl side chain (Scheme 1), are shown in Table II:

$$\ln [\mathrm{VAL}]_t = \ln [\mathrm{VAL}]_0 - k.t \tag{7}$$

$$t_{1/2} = 0.693/k \tag{8}$$

$$\ln (k_{T1}/k_{T2}) = (E_a/R) * (1/T_2 - 1/T_1) \tag{9}$$

The application of the Arrhenius equation (Eq. (9)), where T_1 and T_2 are the absolute reaction temperatures, k_{T1} and k_{T2} are the corresponding rate constants, and R is the universal gas constant, computed an activation energy (E_a) of 10.2 kcal mol^{-1} for the acid degradation process.

HS-MCR Analysis of the Degradation of VAL in Acid Medium

The HS-MCR algorithm was applied to constrain the shape of the concentration profiles obtained by MCR-ALS analysis to fit a first -order kinetic model. This furnished new sets of kinetic profiles and pure spectra of the resolved components (Fig. 4).

Only two components were detected in the degradation samples, the pure spectra of which were similar to those previously estimated by MCR-ALS; however, the concentration profiles obtained by introducing the kinetic model as a third constraint were sharper and free of instrumental noise, resulting in a better agreement with the proposed first-order degradation pathway, as shown by the r^2 values of the fit, nearing unity. The kinetic rate constants for the acid hydrolysis process of the studied samples under the different conditions, as well as their %LOF and r^2 values, are listed in Table II.

Notably, despite the high similarity between the UV spectra of VAL and DP-3, which resulted in only slight reduction of the recorded absorbances during the hydrolysis, the chemometrics methods were capable of detecting only one acid hydrolysis degradation product. In addition, both suggested a rapid hydrolytic process under the applied stress conditions.

HPLC Study of the Hydrolytic and Photolytic Degradation of VAL

For the sake of comparison, the photodegradation of VAL was monitored by HPLC, which confirmed the formation of two impurities. The chromatograms revealed the time-dependent decrease of the peak area corresponding to VAL with a concomitant increase in the peak response of DP-2. In addition, the peak area of the intermediate DP-1 increased up to a maximum and then decreased as a result of its conversion into DP-2.

The HPLC results of the photolyzed samples confirmed that the photodegradation of VAL followed a sequential first-order kinetics, being interpreted by Eq. (7). The slope of the curve of the semilogarithmic plot of the concentration of VAL against time furnished a rate constant (k_1) for its photodegradation [0.045 ($\pm$ 0.002) min^{-1}], from which the half-life time ($t_{1/2}$) of the process could be estimated as 15.5 $\pm$ 0.8 min, using Eq. (8). These values were in good agreement with those obtained employing the chemometrics methodologies (Table I).

In addition, adjustment of the profile of DP-2 to Eq. (6) yielded $k_2 = 0.022 \pm 0.005$ min^{-1} ($r^2 = 0.9859$), in reasonable agreement with the result provided by HS-MCR (Table I). Overall comparison of the chemometrics and chromatographic approaches signaled HS-MCR as the superior alternative, because it solved this kinetic system with a single

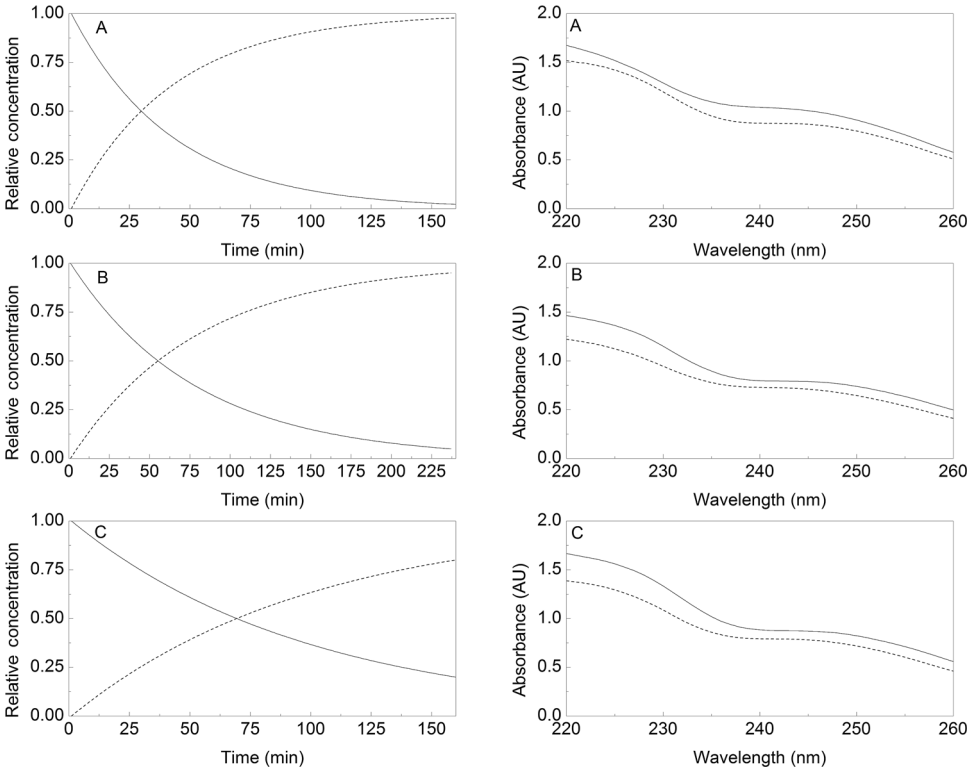

Figure 4 HS-MCR–resolved kinetic profiles and pure spectra obtained in the analysis of individual acid degradation experiments of samples of VAL (0.035 mg mL^{-1}). Left: Concentration profiles of VAL (—) and the degradation product DP-3 (– –). Right: Estimated spectral profiles of VAL (—) and the degradation product DP-3 (– –). (A) In 1.88 N HCl at 85°C. B) In 0.73 N HCl at 85°C. C) In 1.88 N HCl at 65°C.

experiment, being devoid of the rotational ambiguity problem observed in MCR-ALS, which hindered calculation of k_2.

On the other hand, the acid-catalyzed degradation of VAL was also monitored by HPLC (Fig. 5), where the chromatograms exhibited the formation of a single degradation product [11,13]. The semilogarithmic fits of the concentration of VAL against degradation time confirmed a pseudo–first-order degradation kinetics of the hydrolysis, where the evolution of the concentration of VAL at a given time ($[VAL]_t$) could be expressed through Eq. (7). The slopes of the curves obtained by linear regression analysis made possible the calculation of the rate constants (k), and Eq. (8) was used to compute the half-life time ($t_{1/2}$). The application of the Arrhenius equation (Eq. (9)) yielded $E_a = 8.8$ kcal mol^{-1}, confirming the sensitivity of VAL to hydrolysis under acid conditions. The results are given in Table III.

Interestingly, the errors in the determination of the kinetic parameters by the MCR-based determinations were of the same order of magnitude or lower than those obtained by analysis of the HPLC data. This also underscores the advantage of the proposed chemometrics methods over HPLC, since elaboration of a kinetics profile with the latter methodology also requires a much laborious and time-consuming procedure.

The values of E_a suggest that VAL is a moderately acid stable amide; these are similar to those reported for the degradation of polyacrylamide-based systems [29] and amic acid [30], where neighboring groups assist the acid hydrolysis [31]. Thus, it could be inferred that protonation of the neighboring tetrazole moiety of VAL may assist anchimerically the acid hydrolysis of the drug [32]. Interestingly enough, the group of Singh has recently reported that under stress condition VAL hydrolyzes to DP-3 even under neutral conditions [12].

The decomposition of VAL, a polar organic micropollutant, in environmental matrices such as surface waters and urban wastewaters is of high interest [33]. Being a ubiquitous, persistent, and biologically active substance, the presence of VAL in sludge and effluents has provoked recently increasing concern, particularly as there are few or none legal requirements set for its discharge into surface water bodies. In this context, the activation energy and rate constants associated with the degradation of VAL are characteristic parameters that may be useful to better understand the fate of the

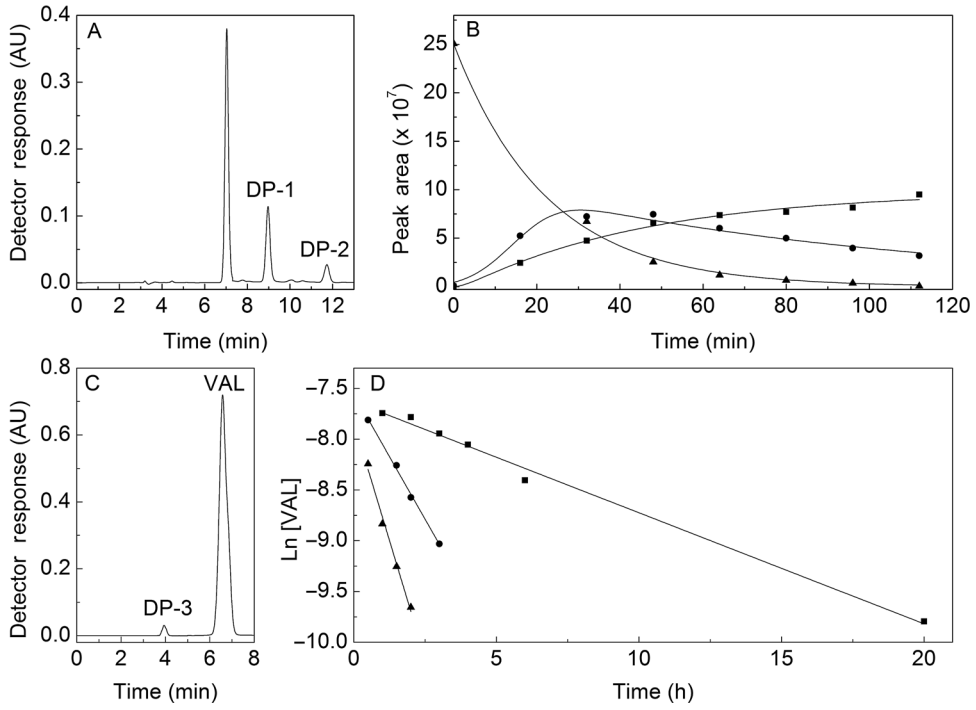

Figure 5 Top: Photodegradation of VAL. (A) Typical chromatogram of VAL and impurities DP-1 and DP-2. (B) Profiles of VAL (▲), DP-1 (●), and DP-2 (■) during the photodegradation of VAL. Bottom: Degradation of VAL in acid medium. (C) Typical HPLC run of the separation of DP-3 and VAL. (D) Semilogarithmic plots of the degradation of VAL, when exposed to 0.49 N HCl at 42°C (■) and 100°C (▲) and when treated with 0.11 N HCl at 100°C (●).

Table III HPLC-Derived Parameters, Characterizing the Acid Degradation Kinetics of VAL[a]

HCl (N)	Temperature (°C [K])	k (min^{-1})	$t_{1/2}$ (min)
0.49	100.0 [373]	0.016 (1)	43 (3)
0.49	42.0 [315]	0.0018 (7)	385 (15)
0.11	100.0 [373]	0.0082 (3)	85 (3)

[a]Numbers in parentheses indicate the standard deviations of the determinations at the last significant digits level.

drug in the environment [34]. In addition, the proposed chemometrics approach may be employed as an advantageous alternative for characterizing the degradation of VAL under different conditions.

CONCLUSIONS

This work demonstrated the suitability of hard and soft modeling multivariate curve resolution methods for the study of a drug degradation process under stress conditions. The application of MCR-ALS and HS-MCR methodologies furnished detailed descriptions of the kinetics of the acid and photoneutral degradation of VAL, making it possible to estimate the pure spectra of the degradation products and, at the same time, to determine their concentration profiles and the degradation rate constants of the drug under the different conditions. In the photodegradation scenario, the HS-MCR modeling exhibited superior performance than the MCR-ALS algorithm, providing better adjustment of the data to the proposed kinetic models. The quality of the results was confirmed by independent HPLC analysis of degraded samples.

The authors thank the National University of Rosario (UNR), Secretary of Science, Technology and Innovation (SECTeI), Argentine National Research Council (CONICET), and National Agency for the Promotion of Science and Technology (ANPCyT) for financial support and a fellowship (RMB). We also thank Dr. D. Casas (Laboratorios Lazar, Argentine) for the kind provision of Valsartan and Drs. J. M. Amigo and A. de Juan for providing a copy of HS-MCR.

BIBLIOGRAPHY

1. Massart, D.; Vandeginste, B.; Buydens, L.; De Jong, S.; Lewi, P.; Smeyers-Verbeke, J. Handbook of

Chemometrics and Qualimetrics; Elsevier: Amsterdam, The Netherlands, 1998.
2. Brereton, R. G.; Booth, D. E. Chemometrics, Data Analysis for the Laboratory and Chemical Plant; Wiley: Chichester, UK, 2003.
3. de Juan, A.; Casassas, E.; Tauler, R. In Encyclopedia of Analytical Chemistry: Applications, Theory and Instrumentation; Meyers, R. A., Ed.; Wiley: New York, 2000.
4. de Juan, A.; Maeder, M.; Martínez, M.; Tauler, R. Chemometr Intell Lab Syst 2000, 54, 123–141.
5. Mistry, N. B.; Westheim, A. S.; Kjeldsen, S. E. Expert Opin Pharmacother 2006, 7, 575–581.
6. Görog, S. In Identification and Determination of Impurities in Drugs; Elsevier: Amsterdam, The Netherlands, 2000; Vol. 4, Chap. 5.
7. ICH Q1A(R2). Stability Testing of New Drug Substances and Products. International Conference on Harmonisation of Technical Requirements for Registration of Pharmaceuticals for Human Use, Geneva, Switzerland, 2003.
8. Baertschi, S. W.; Alsante, K. M.; Reed, R. A. Pharmaceutical Stress Testing: Predicting Drug Degradation, 2nd ed.; Taylor & Francis: New York, 2011.
9. Agrahari, V.; Kabra, V.; Gupta, S.; Kumar Nema, R.; Nagar, M.; Karthikeyan, C.; Trivedi, P. Int J Pharm Clin Res 2009, 1, 77–81.
10. Rao, K. S.; Jena, N.; Rao, M. E. B. J Young Pharm 2010, 2, 183–189.
11. Bianchini, R. M.; Castellano, P. M.; Kaufman, T. S. J Liq Chromatogr Relat Technol 2012, 35, 1053–1069.
12. Mehta, S.; Shah, R. P.; Singh, S. Drug Test Anal 2010, 2, 82–90.
13. Bianchini, R. M.; Castellano, P. M.; Kaufman, T. S. J Pharm Biomed Anal 2011, 56, 16–22.
14. Krishnaiah, Ch.; Raghupathi Reddy, A.; Kumar, R.; Mukkanti, K. J Pharm Biomed Anal 2010, 53, 483–489.
15. Jaumot, J.; Gargallo, R.; de Juan, A.; Tauler, R. Chemometr Intell Lab Syst 2005, 76, 101–110.
16. United States Pharmacopeial Convention. The United States Pharmacopoeia, 32th ed.; Rockville, MD, 2009.
17. Jiang, J. H.; Liang Y.; Ozaki, Y. Chemometr Intell Lab Syst 2004, 71, 1–12.
18. Tauler, R. J Chemometr 2001, 15, 627–646.
19. Golub, G. H.; Van Loan, C. F. Matrix Computations, 2nd ed.; The John Hopkins University Press: London, UK, 1989.
20. Tauler, R.; Durand, G.; Barceló, D. Chromatographia 1992, 33, 244–254.
21. Sánchez, F. C.; Toft, J.; van den Bogaert, B.; Massart, D. L. Anal Chem 1996, 68, 79–85.
22. Bro, R.; De Jong, S. J Chemometr 1997, 11, 393–401.
23. Tauler, R. Chemometr Intell Lab Syst 1995, 30, 133–146.
24. Malinowski, E. R. Factor Analysis in Chemistry, 3rd ed.; Wiley: New York, 2002, p. 495.
25. De Luca, M.; Mas, S.; Ioele, G.; Oliverio, F.; Ragno, G.; Tauler, R. Int J Pharm 2010, 386, 99–107.
26. Muñoz, G.; de Juan, A. Anal Chim Acta 2007, 595, 198–208.
27. Tauler, R.; Smilde, A. K.; Kowalski, B. R. J Chemometr 1995, 9, 31–58.
28. Jones, C. T.; Banks, P. Biochem J 1970, 118, 801–810.
29. Al-Muntasheri, G. A.; Nasr-El-Din, H. A.; Peters, J. A.; Zitha, P. L. J. Eur Polymer J 2008, 44, 1225–1237.
30. Gopala Krishnan, P. S.; Vora, R. H.; Chung, T. S. Polymer 2001, 42, 5165–5174.
31. Signor, A.; Bordignon, E.; Vidali, G. J Org Chem 1967, 32, 1135–1139.
32. Tosco, P.; Rolando, B.; Fruttero, R.; Henchoz, Y.; Martel, S.; Carrupt, P. A.; Gasco, A. Helv Chim Acta 2008, 91, 468–482.
33. Kern, S.; Baumgartner, R.; Helbling, D. E.; Hollender, J.; Singer, H.; Loos, M. J.; Schwarzenbach, R. P.; Fenner, K. J Environ Monitor 2010, 12, 2100–2111.
34. Yang, H.; Li, G.; An, T.; Gao, Y.; Fu, J. Catal Today 2010, 153, 200–207.